# Bypassing a Kinase Activity with an ATP-Competitive Drug

Feroz R. Papa,[1,3]* Chao Zhang,[2] Kevan Shokat,[2] Peter Walter[3,4]

**Unfolded proteins in the endoplasmic reticulum cause trans-autophosphorylation of the bifunctional transmembrane kinase Ire1, which induces its endoribonuclease activity. The endoribonuclease initiates nonconventional splicing of *HAC1* messenger RNA to trigger the unfolded-protein response (UPR). We explored the role of Ire1's kinase domain by sensitizing it through site-directed mutagenesis to the ATP-competitive inhibitor 1NM-PP1. Paradoxically, rather than being inhibited by 1NM-PP1, drug-sensitized Ire1 mutants required 1NM-PP1 as a cofactor for activation. In the presence of 1NM-PP1, drug-sensitized Ire1 bypassed mutations that inactivate its kinase activity and induced a full UPR. Thus, rather than through phosphorylation per se, a conformational change in the kinase domain triggered by occupancy of the active site with a ligand leads to activation of all known downstream functions.**

Secretory and transmembrane proteins traversing the endoplasmic reticulum (ER) during their biogenesis fold to their native states in this compartment (*1*). This process is facilitated by a plethora of ER-resident activities (the protein folding machinery) (*2*). Insufficient protein folding capacity causes an accumulation of unfolded proteins in the ER lumen (a condition referred to as ER stress) and triggers a transcriptional program called the UPR. In yeast, UPR targets include genes encoding chaperones, oxido-reductases, phospholipid biosynthetic enzymes, ER-associated degradation components, and proteins functioning downstream in the secretory pathway (*3*). Together, UPR target activities afford proteins passing through the ER an extended opportunity to fold and assemble properly, dispose of unsalvageable unfolded polypeptides, and increase the capacity for ER export.

The yeast UPR is signaled through the ER stress sensor Ire1, a single-spanning ER transmembrane protein with three functional domains (*4*). The most N-terminal domain, which resides in the ER lumen, senses elevated levels of unfolded ER proteins. Dissociation of ER chaperones from Ire1 as they become engaged with unfolded proteins is thought to trigger Ire1 activation (*3*).

Ire1's most C-terminal domain is a regulated endoribonuclease (RNase), which has a single known substrate in yeast: the *HAC1*$^u$ mRNA (u stands for uninduced), which encodes the Hac1 transcriptional activator necessary for activation of UPR targets (*5*). *HAC1*$^u$ mRNA is constitutively transcribed, but not translated, because it contains a nonconventional translation-inhibitory intron (*6*). Upon activation, Ire1's RNase cleaves *HAC1*$^u$ mRNA at two specific sites, excising the intron (*7*). The 5′ and 3′ exons are rejoined by tRNA ligase (*8*), resulting in spliced *HAC1*$^i$ mRNA (i stands for induced), which is actively translated to produce the Hac1 transcriptional activator, in turn upregulating UPR target genes (*5*).

A functional kinase domain precedes the RNase domain on the cytosolic side of the ER membrane (*9*). Activation of Ire1 leads to its oligomerization in the ER membrane, followed by trans-autophosphorylation (*9*, *10*). Mutations of catalytically essential kinase active-site residues or mutations of residues known to become phosphorylated prevent *HAC1*$^u$ mRNA splicing and abrogate UPR signaling, demonstrating that Ire1's kinase phosphotransfer function is essential for RNase activation (*4*, *9*, *11*). Thus, Ire1 communicates an unfolded-protein signal from the ER to the cytosol using the lumenal domain as the sensor and the RNase domain as the effector. Although clearly important for the circuitry of this machine, it is unknown why and how Ire1's kinase is required for activation of its RNase. To dissect the role of Ire1's kinase function, we used a recently developed strategy that allows us to sensitize Ire1 to specific kinase inhibitors (*12*).

**Unexpected behavior of Ire1 mutants sensitized to an ATP-competitive drug.** The mutation of Leu$^{745}$—situated at a conserved position in the adenosine 5′-triphosphate (ATP)–binding site—to Ala or Gly is predicted to sensitize Ire1 to the ATP-competitive drug 1-tert-butyl-3-naphthalen-1-ylmethyl-1*H*-pyrazolo[3,4-*d*]pyrimidin-4-ylemine (1NM-PP1) by creating an enlarged active-site pocket not found in any wild-type kinase (*13*). Most kinases are not affected by these mutations, but others are partially or severely impaired (*14*, *15*). For Ire1, these substitutions markedly decreased UPR signaling (assayed through an in vivo reporter), which is indicative of decreased kinase activity. Ire1(L$^{745}$→A$^{745}$) [Ire1(L745A) (*16*)] showed a 40% decrease relative to the wild-type kinase, whereas Ire1(L745G) showed a >90% decrease, approaching that of the Δ*ire1* control (Fig. 1A).

Unexpectedly, the addition of 1NM-PP1 to cells expressing partially active Ire1(L745A) caused no inhibition, even at concentrations that completely inhibit other 1NM-PP1–sensitized kinases (*15*, *17*). Instead, 1NM-PP1 increased reporter activity slightly (Fig. 1A, bar 4). To our further surprise, 1NM-PP1 provided significantly restored signaling to the severely crippled Ire1(L745G) (Fig. 1A, bar 6). This result presents a paradox: An ATP-competitive compound that was expected to function as an inhibitor of the rationally engineered mutant enzyme instead permits activation.

UPR activation strictly required induction by dithiothreitol (DTT) (Fig. 1) or tunicamycin (*18*); 1NM-PP1 by itself had no effect, indicating that it does not induce the UPR by directly affecting ER protein folding. Moreover, the effects of 1NM-PP1 were specific: other structurally similar compounds, 2-naphthylmethyl PP1, which is a regio-isomer, and 1-naphthyl PP1, which lacks the methylene group between the heterocyclic ring and the naphthyl group, neither activated nor inhibited wild-type or mutant Ire1 (*18*).

Activation rather than inhibition by an ATP-competitive inhibitor raised the question of whether the kinase activity is necessary in the 1NM-PP1–sensitized mutants. To this end, we combined the L745A or L745G mutation with a "kinase-dead" variant D828A, which lacks an active-site Asp residue needed to chelate $Mg^{2+}$ (*11*, *19*). Whereas the Ire1(L745A,D828A) double mutant was detectable in cells at levels near those of wild-type cells, Ire1(L745G,D828A) was undetectable, probably because of instability, and could not be assayed. As expected, Ire1(L745A,D828A) was unable to induce the UPR reporter with DTT alone, but the addition of 1NM-PP1 allowed activation to levels approaching 80% of the wild-type activation level (Fig. 1B). This suggests that the binding of 1NM-PP1 to 1NM-PP1–sensitized Ire1 renders the kinase activity dispensable.

[1]Department of Medicine, [2]Department of Cellular and Molecular Pharmacology, [3]Department of Biochemistry and Biophysics, [4]Howard Hughes Medical Institute, University of California, San Francisco, CA 94143–2200, USA.

*To whom correspondence should be addressed. E-mail: frpapa@medicine.ucsf.edu

Trans-autophosphorylation by Ire1 of two activation-segment Ser residues ($S^{840}$ and $S^{841}$) is necessary for signaling (*9*), prompting the question of whether this requirement is also bypassed in 1NM-PP1–sensitized mutants. As expected, the unphosphorylatable Ire1 (S840A,S841A) mutant was inactive in the absence and presence of 1NM-PP1 (Fig. 1C). In contrast, the 1NM-PP1–sensitized Ire1 (L745A,S840A,S841A) and Ire1(L745G, S840A,S841A) mutants were significantly activated by 1NM-PP1, indicating that phosphorylation of $S^{840}$ and $S^{841}$ can be bypassed. Two trends are apparent: With DTT alone, relative to the parent mutant Ire1(S840A,S841A), signaling decreased as the side chain of residue 745 was progressively reduced from Leu to Ala to Gly (Fig. 1C, bars 3, 5, and 7). This is consistent with the results of Fig. 1A, which show an increasing sensitivity of the active-site to side-chain reduction at residue 745. Reciprocally, in the presence of 1NM-PP1, activation of 1NM-PP1–sensitized Ire1(S840A,S841A) mutants increased in the same order (Fig. 1C, bars 4, 6, and 8), perhaps because of progressively enhanced binding by 1NM-PP1 as the residue 745 side chain was trimmed back.

**1NM-PP1–sensitized Ire1 requires 1NM-PP1 as a cofactor for *HAC1* mRNA splicing.** We next confirmed that activation by 1NM-PP1–sensitized Ire1 mutants followed the expected pathway of activating *HAC1* mRNA splicing and Hac1 protein production. As expected, UPR induction of wild-type cells with DTT caused splicing of *HAC1* mRNA, as revealed by near-complete conversion of $HAC1^u$ to $HAC1^i$ mRNA (Fig. 2A, lanes 1 and 2) (*5*); 1NM-PP1 had no effect by itself or with DTT (Fig. 2A, lanes 3 and 4). In strict correlation with *HAC1* mRNA splicing, Hac1 protein accumulated significantly (Fig. 2C, lanes 2 and 4).

In contrast, cells expressing 1NM-PP1–sensitized Ire1(L745G) spliced *HAC1* mRNA weakly with DTT alone, but displayed a significant increase when 1NM-PP1 was also provided (Fig. 2A, lanes 5 to 8). 1NM-PP1 alone did not activate *HAC1* mRNA splicing. As expected, Hac1 protein levels correlated with splicing (e.g., Fig. 2C, lanes 6 and 8). Activation by 1NM-PP1 was even more pronounced in cells expressing the Ire1(L745A,D828A) double mutant, which neither spliced *HAC1* mRNA nor produced Hac1 protein with DTT alone, but exhibited robust splicing and Hac1 protein production when provided both 1NM-PP1and DTT (Fig. 2, A and C, compare lanes 10 and 12).

Importantly, steady-state levels of Ire1 proteins were comparable in all experiments, excluding as a trivial explanation for the observed effects the possibility that 1NM-PP1–sensitized Ire1 mutants are only stably expressed in the presence of 1NM-PP1 (Fig. 2D). Taken together, our data show that 1NM-PP1 permits but does not instruct 1NM-PP1–sensitized Ire1 mutants to splice *HAC1* mRNA in response to ER stress. Thus, in the genetic background of 1NM-PP1–sensitized *IRE1* alleles, 1NM-PP1 is, in effect, a cofactor for signaling in the UPR.

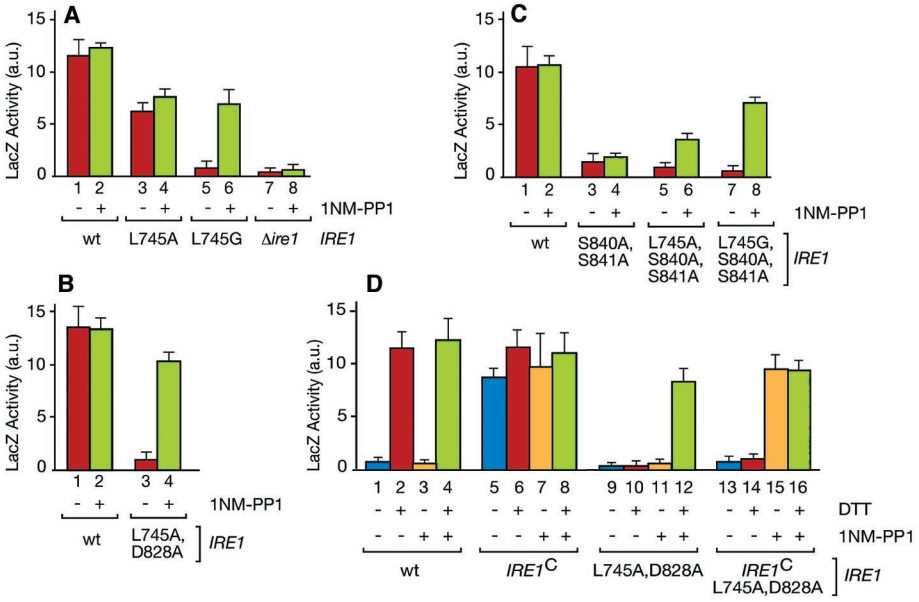


**Fig. 1.** (**A** to **D**) In vivo UPR assays using a UPR element–driven *lacZ* reporter. The relevant genotypes and the presence or absence of 1NM-PP1 and the UPR inducer DTT are indicated. For (A) to (C), DTT was used in all assays. wt, wild type; a.u., arbitrary units.

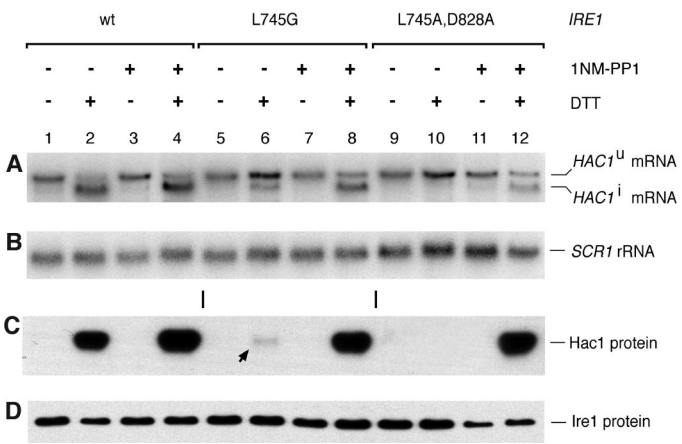


**Fig. 2.** In vivo *HAC1* mRNA splicing and Hac1 protein production. Northern blots showing (**A**) in vivo *HAC1* mRNA splicing and (**B**) *SCR1* ribosomal RNA (rRNA) as loading control. Western blots showing (**C**) Hac1 and (**D**) Ire1 protein levels. The arrow in (C), lane 6, calls attention to the small amount of Hac1 protein present in these cells.

**1NM-PP1 uncouples the kinase and RNase activities of 1NM-PP1–sensitized Ire1.** To rule out indirect effects, we assayed the activities of the Ire1 mutants described above in vitro. The cytosolic portion of Ire1 consisting of the kinase domain and RNase domain (Ire1*) was expressed and purified from *Escherichia coli* (*7*). Using [$\gamma$-$^{32}$P]-labeled ATP, we assayed wild-type Ire1* and Ire1*(L745G) for autophosphorylation in the presence or absence of 1NM-PP1. Wild-type Ire1* exhibited strong autophosphorylation, which was not inhibited by 1NM-PP1 (Fig. 3A, lanes 1 and 2). In contrast, Ire1*(L745G) exhibited markedly diminished autophosphorylation, consistent with poor signaling by Ire1(L745G) in vivo (Figs. 1 and 2), which was completely extinguished by 1NM-PP1 (Fig. 3A, lane 3 and 4). This suggested that Ire1*(L745G) is diminished in its ability to use ATP as substrate and that 1NM-PP1 is, as predicted, an ATP competitor.

In contrast, when provided with [$\gamma$-$^{32}$P]-labeled *N*-6 benzyl ATP, an ATP analog with a bulky substituent (Fig. 3E), Ire1*(L745G) displayed enhanced autophosphorylation activity relative to wild-type Ire1* (Fig. 3B, lane 1 and 2). Therefore, the L745G mutation does not destroy Ire1's catalytic function, but rather alters its substrate specificity from ATP to ATP analogs having complementary features that permit binding in the expanded active site.

To ask how the RNase activity of Ire1 is affected by manipulation of its kinase domain, we incubated wild-type Ire1* and Ire1*(L745G) with a truncated in vitro transcribed *HAC1* RNA substrate ($HAC1_{600}$) and monitored the production of cleavage products (*7*). Wild-type Ire1* cleaved $HAC1_{600}$ RNA at both splice junctions, producing the expected fragments corresponding to the singly and doubly cut species (Fig. 3C,

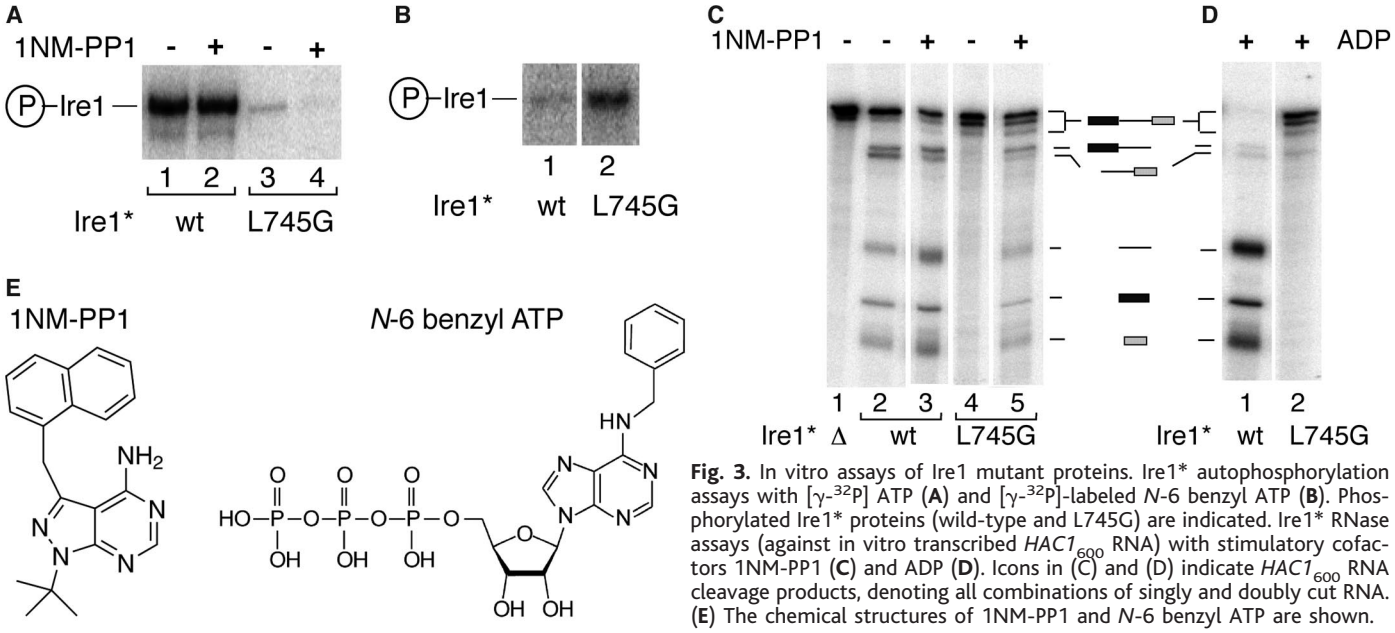


**Fig. 3.** In vitro assays of Ire1 mutant proteins. Ire1* autophosphorylation assays with [$\gamma$-$^{32}$P] ATP (**A**) and [$\gamma$-$^{32}$P]-labeled *N*-6 benzyl ATP (**B**). Phosphorylated Ire1* proteins (wild-type and L745G) are indicated. Ire1* RNase assays (against in vitro transcribed $HAC1_{600}$ RNA) with stimulatory cofactors 1NM-PP1 (**C**) and ADP (**D**). Icons in (C) and (D) indicate $HAC1_{600}$ RNA cleavage products, denoting all combinations of singly and doubly cut RNA. (**E**) The chemical structures of 1NM-PP1 and *N*-6 benzyl ATP are shown.

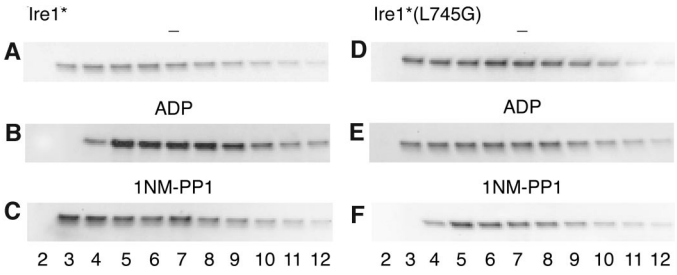


**Fig. 4.** Glycerol-density gradient velocity sedimentation of wild-type and mutant Ire1*. Ire1* proteins (**A** to **C**) and Ire1*(L745G) proteins (**D** to **F**) were incubated in the presence of ADP [(B) and (E)] or 1NM-PP1 [(C) and (F)] and subjected to velocity sedimentation analysis. Sedimentation is from left to right.

lane 2). The cleavage reaction was not affected by 1NM-PP1 (Fig. 3C, lane 3). In contrast, Ire1*(L745G) was completely inactive, whereas the addition of 1NM-PP1, at the same concentration that was shown in Fig. 3A (lane 4) to completely inhibit the kinase activity, restored RNase activity significantly (Fig. 3C, lanes 4 and 5), strongly supporting the notion that 1NM-PP1 uncouples the kinase and RNase activities of 1NM-PP1–sensitized Ire1.

We have previously shown that cleavage of *HAC1* mRNA by wild-type Ire1* is stimulated by adenosine 5′-diphosphate (ADP) (*7*). This is consistent with the notion derived from in vivo studies that Ire1 requires an active kinase domain, because we know that recombinant wild-type Ire1* is already phosphorylated, thereby alleviating a necessity for de novo phosphorylation in vitro. ADP efficiently stimulated the RNase activity of Ire1* (Fig. 3D, lane 1) but not that of Ire1*(L745G) (Fig. 3D, lane 2).

For wild-type Ire1 and 1NM-PP1–sensitized Ire1(L745G), ADP and 1NM-PP1, respectively, function as stimulatory cofactors. Therefore, we asked whether a conformational change occurs in response to cofactor binding by analyzing Ire1* and Ire1*(L745G) through glycerol-gradient velocity sedimentation. Ire1* sedimented as a broad peak in the gradient (Fig. 4). Upon the addition of ADP (Fig. 4B), but not 1NM-PP1 (Fig. 4C), the peak of Ire1* shifted as a result of faster sedimentation. Conversely, the peak of Ire1*(L745G) shifted by a corresponding amount upon the addition of 1NM-PP1 (Fig. 4F) but not upon the addition of ADP (Fig. 4E). This shift may be indicative of a conformational change and/or change in the oligomeric state of the enzymes in response to the binding of their respective cofactors.

**1NM-PP1–sensitized, kinase-dead Ire1 signals a canonical UPR.** To ask whether bypassing the Ire1 kinase activity with 1NM-PP1 allows the induction of a full UPR, we profiled mRNA expression on yeast genomic microarrays. To this end, mRNA from wild-type *IRE1*, Δ*ire1*, and *IRE1*(L745A,D828A) cells was isolated at different points in time after the addition of 1NM-PP1 and DTT. cDNAs derived from these mRNA populations were labeled with different fluorescent dyes, mixed pairwise, and hybridized to microarrays (*20*). Scatter plots of pairwise comparisons of mRNA expression levels are shown in Fig. 5; the *x*-*y* scatter plots represent relative expressions for every mRNA between the specified genotypes.

The comparison of wild-type *IRE1*-expressing cells with Δ*ire1* cells revealed a distinct set of up-regulated UPR target genes in wild-type *IRE1*-expressing cells (Fig. 5A; genes that were up-regulated more than twofold are shown in pink). These *IRE1*-dependent genes include previously described UPR transcriptional targets (*21*, *22*). Notably, the same set of (pink-colored) UPR target genes was up-regulated to a similar magnitude in *IRE1*(L745A,D828A)-expressing cells relative to Δ*ire1* cells (Fig. 5B), suggesting that a canonical UPR was induced in the 1NM-PP1–sensitized, kinase-dead mutant. This conclusion was confirmed by the tight superimposition of the scatter diagonals of both UPR targets and the rest of the transcriptome evident in the expression profiles of wild-type *IRE1*- compared with *IRE1*(L745A,D828A)-expressing cells (Fig. 5C).

**Building an instructive UPR switch.** The 1NM-PP1–sensitized *IRE1* mutants described so far act permissively, because activation requires both 1NM-PP1 and protein-misfolding agents. This indicates that an unfolded-protein signal needs to be received by the ER lumenal domain for activation. We asked if we could bypass this requirement using a constitutively on version of *IRE1* (called $IRE1^C$) isolated previously through random mutagenesis of the ER lumenal domain (*18*, *21*). $IRE1^C$ significantly induced the UPR without DTT, resulting in about 75% of the maximal activity of wild-type *IRE1* with DTT (Fig. 1D, bars 2 and 5). We predicted that a chimera of the $IRE1^C$ and 1NM-PP1–sensitized, kinase-dead *IRE1*(L745A,D828A) mutants would activate the UPR with 1NM-PP1 alone, even in the absence of DTT. The data in Fig. 1D (bars 13 to 16) show that this prediction holds

true. Whereas wild-type *IRE1* requires DTT for induction and is immune to 1NM-PP1 (Fig. 1D, bars 1 to 4), and *IRE1*(L745A,D828A) requires both DTT and 1NM-PP1 (Fig. 1D, bars 9 to 12), the chimeric $IRE1^{C}$ (L745A,D828A) requires only 1NM-PP1 for activation, irrespective of the addition of DTT (Fig. 1D, bars 13 to 16). Thus, $IRE1^{C}$ (L745A,D828A) is an instructive switch that turns on the UPR upon the addition of 1NM-PP1 alone (i.e., even in the absence of ER stress).

**Summary and implications.** Since our discovery that Ire1's RNase initiates splicing of *HAC1* mRNA, the function of its kinase domain has remained an enigma (*7*). Although mutational analyses have indicated a requirement for an enzymatically active kinase and have defined activation-segment phosphorylation sites (*9*), to date no targets besides Ire1 itself have been identified. Here, we report that both the kinase activity and activation-segment phosphorylation can be bypassed if the small ATP-mimic 1NM-PP1 is provided to a mutant enzyme to which it can bind. Instead of inhibiting the function served by ATP, 1NM-PP1 rectifies the signaling defect of 1NM-PP1–sensitized Ire1 mutants, leading to the induction of a canonical UPR (*21*). Thus, ligand binding to the kinase domain, rather than a phosphotransfer function mediated by the kinase activity, is required for RNase activation. The kinase module of Ire1, therefore, uses an unprecedented mechanism to propagate the UPR signal.

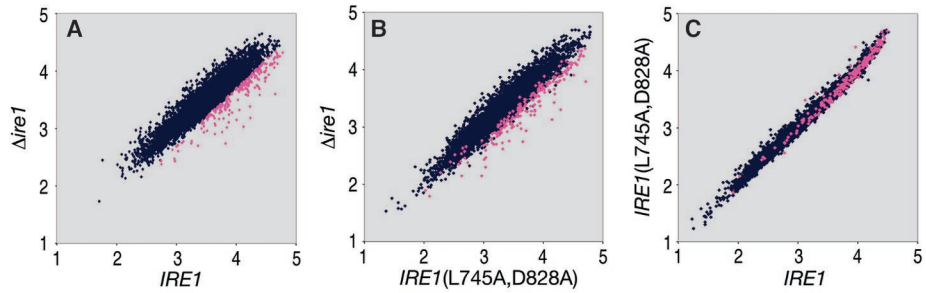


**Fig. 5.** (**A** to **C**) *x-y* scatter plot analysis of mRNA abundance. The plots ($log_{10}$) compare yeast genomic microarray analyses between the genotypes indicated. In each case, mRNA was purified from cells that were provided both DTT and 1NM-PP1. Pink dots represent genes with expression more than two times as high in wild-type cells as in Δ*ire1* cells.

One model that could explain our data is proposed in Fig. 6B. According to this model, autophosphorylation of wild-type Ire1 occurs in trans between Ire1 molecules after they have been released from their chaperone anchors and have oligomerized by lateral diffusion in the plane of the ER membrane (*9*, *23*). Trans-autophosphorylation of the activation segment locks the activation segment in the "swung-out" state (*24*, *25*), and fully opens the active site, allowing ADP or ATP to bind efficiently, leading in turn to conformational changes that activate the RNase domain.

In contrast, the binding of 1NM-PP1 to the active site of 1NM-PP1–sensitized Ire1 occurs even in the absence of phosphorylation of the activation segment. It is plausible that because of its small size, 1NM-PP1 can bypass the "closed" activation segment, which is proposed to occlude access to the active site for the larger ADP and ATP molecules (Fig. 6A). Alternatively, 1NM-PP1 may enter the active site when the unphosphorylated activation segment opens transiently, which occurs with low frequency in other kinases (*26*). If the off-rate of 1NM-PP1 binding to 1NM-PP1–sensitized Ire1 is slow compared to that of ADP and ATP, most mutant Ire1 molecules could be trapped in a drug-bound state. Based on either scenario, we propose that drug binding alone causes conformational rearrangements in the kinase that activate the RNase. The nucleotide-bound state of phosphorylated wild-type Ire1, therefore, mimics the 1NM-PP1–bound state of unphosphorylated 1NM-PP1–sensitized Ire1.

The model discussed so far does not explain why 1NM-PP1 should not bind to individual 1NM-PP1–sensitized Ire1 molecules and activate them, even without oligomerization induced by activation of the UPR through the ER lumenal domain. Two possibilities could account for the observations: (i) The binding of 1NM-PP1 may be enhanced in oligomerized, chaperone-free mutants, or (ii) 1NM-PP1 may bind equally well to chaperone-anchored and chaperone-free (or constitutive-on) Ire1, but oligomerization may be required because interaction between neighboring molecules is required for the conformational change that activates the RNase

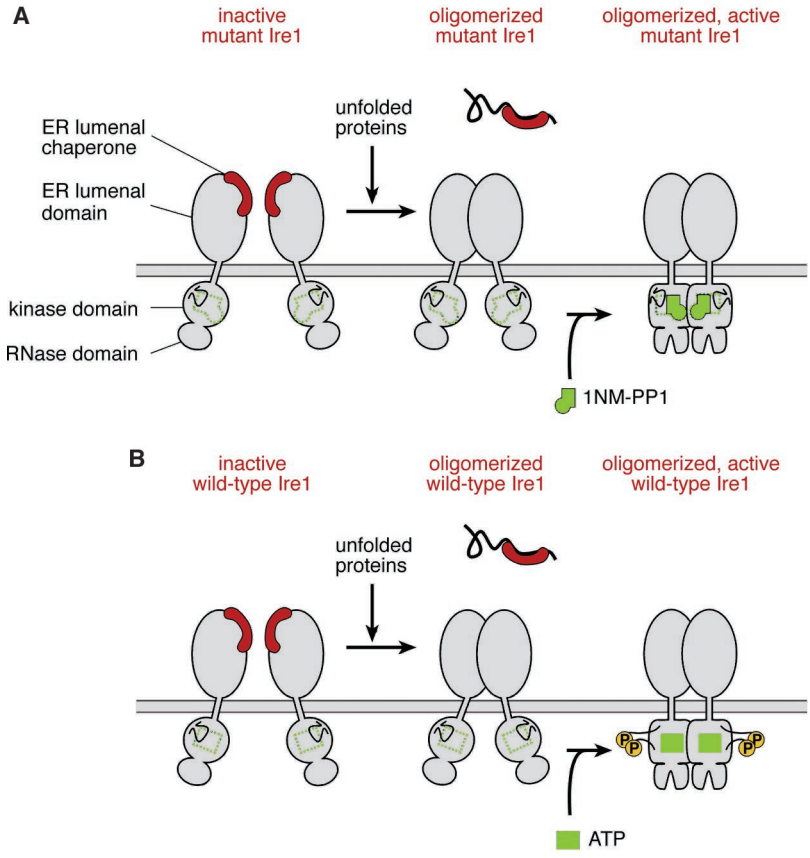


**Fig. 6.** Model of activation of 1NM-PP1–sensitized and wild-type Ire1. For both proteins, chaperone dissociation resulting from unfolded-protein accumulation causes oligomerization in the plane of the ER membrane, which is a precondition for further activation. For mutant Ire1 (**A**), 1NM-PP1 binding to the inactive kinase domain active site causes a conformational change, which activates the RNase. For wild-type Ire1 (**B**), trans-autophosphorylation, with ATP, of the activation segment fully opens the kinase domain for binding of ADP or ATP, which activates the RNase.

function. Currently, our data do not allow us to distinguish between these possibilities.

Our findings provoke the question of what the "natural" stimulatory ligand of Ire1's kinase domain may be. One likely candidate is ADP, which is generated by Ire1 from ATP during the autophosphorylation reaction. In vitro, ADP is a better activator of Ire1 than ATP (*7*). Ire1 would therefore be "self priming," generating an efficient activator already bound to its active site. In many professional secretory cells such as the β-cells of the endocrine pancreas (which contain high concentrations of Ire1), ADP levels rise (and ATP levels decline) temporarily in proportion to nutritional stress (*27*). ADP therefore is physiologically poised to serve as a cofactor that could signal a starvation state. It is known that protein folding becomes inefficient as the nutritional status of cells declines, triggering the UPR (*28*). Thus, in the face of ATP depletion, ADP-mediated conformational changes might increase the dwell time of activated Ire1. As such, Ire1 could have evolved this regulatory mechanism to monitor the energy balance of the cell and couple this information to activation of the UPR.

Although unprecedented in proteins containing active kinase domains, our findings are consistent with previous observations of RNase L, which is closely related to Ire1, bearing a kinase-like domain followed C-terminally by an RNase domain (*29*, *30*). Similar to Ire1, RNase L is activated by dimerization (*31*). However, RNase L's kinase domain is naturally inactive (*29*), whereas its RNase activity is stimulated by adenosine nucleotide binding to the kinase domain. Therefore, like Ire1, the ligand-occupied kinase domain of RNase L serves as a module that participates in activation and regulation of the RNase function. Insights gained from Ire1 and RNase L may extend to other proteins containing kinase or enzymatically inactive pseudokinase domains (*32*).

### References and Notes


1. M. J. Gething, J. Sambrook, *Nature* **355**, 33 (1992).
2. F. J. Stevens, Y. Argon, *Semin. Cell Dev. Biol.* **10**, 443 (1999).
3. C. Patil, P. Walter, *Curr. Opin. Cell Biol.* **13**, 349 (2001).
4. J. S. Cox, C. E. Shamu, P. Walter, *Cell* **73**, 1197 (1993).
5. J. S. Cox, P. Walter, *Cell* **87**, 391 (1996).
6. U. Ruegsegger, J. H. Leber, P. Walter, *Cell* **107**, 103 (2001).
7. C. Sidrauski, P. Walter, *Cell* **90**, 1031 (1997).
8. C. Sidrauski, J. S. Cox, P. Walter, *Cell* **87**, 405 (1996).
9. C. E. Shamu, P. Walter, *EMBO J.* **15**, 3028 (1996).
10. A. Weiss, J. Schlessinger, *Cell* **94**, 277 (1998).
11. K. Mori, W. Ma, M. J. Gething, J. Sambrook, *Cell* **74**, 743 (1993).
12. K. Shah, Y. Liu, C. Deirmengian, K. M. Shokat, *Proc. Natl. Acad. Sci. U.S.A.* **94**, 3565 (1997).
13. A. C. Bishop *et al.*, *Curr. Biol.* **8**, 257 (1998).
14. E. L. Weiss, A. C. Bishop, K. M. Shokat, D. G. Drubin, *Nature Cell Biol.* **2**, 677 (2000).
15. A. C. Bishop *et al.*, *Nature* **407**, 395 (2000).
16. Single-letter abbreviations for the amino acid residues are as follows: A, Ala; D, Asp; G, Gly; L, Leu; and S, Ser.
17. A. S. Carroll, A. C. Bishop, J. L. DeRisi, K. M. Shokat, E. K. O'Shea, *Proc. Natl. Acad. Sci. U.S.A.* **98**, 12578 (2001).
18. F. R. Papa, C. Zhang, K. Shokat, P. Walter, data not shown.
19. M. Huse, J. Kuriyan, *Cell* **109**, 275 (2002).
20. J. L. DeRisi, V. R. Iyer, P. O. Brown, *Science* **278**, 680 (1997).
21. K. J. Travers *et al.*, *Cell* **101**, 249 (2000).
22. Materials and methods are available as supporting material on *Science* Online.
23. F. Urano, A. Bertolotti, D. Ron, *J. Cell Sci.* **113**, 3697 (2000).
24. S. R. Hubbard, M. Mohammadi, J. Schlessinger, *J. Biol. Chem.* **273**, 11987 (1998).
25. T. Schindler *et al.*, *Mol. Cell* **3**, 639 (1999).
26. M. Porter, T. Schindler, J. Kuriyan, W. T. Miller, *J. Biol. Chem.* **275**, 2721 (2000).
27. F. Schuit, K. Moens, H. Heimberg, D. Pipeleers, *J. Biol. Chem.* **274**, 32803 (1999).
28. R. J. Kaufman *et al.*, *Nature Rev. Mol. Cell Biol.* **3**, 411 (2002).
29. B. Dong, M. Niwa, P. Walter, R. H. Silverman, *RNA* **7**, 361 (2001).
30. S. Naik, J. M. Paranjape, R. H. Silverman, *Nucleic Acids Res.* **26**, 1522 (1998).
31. B. Dong, R. H. Silverman, *Nucleic Acids Res.* **27**, 439 (1999).
32. M. Kroiher, M. A. Miller, R. E. Steele, *Bioessays* **23**, 69 (2001).


33. We thank M. Stark for constructing the *IRE1*$^{C}$ allele, S. Ullrich for his initial effort in constructing Ire1 mutants, and J. Kuriyan and members of the Walter and Shokat labs for valuable discussions. Supported by grants from the NIH to P.W. (GM32384) and K.S. (AI44009), and postdoctoral support from the UCSF Molecular Medicine Program (to F.P.). P.W. receives support as an investigator of the Howard Hughes Medical Institute.


**Supporting Online Material**

www.sciencemag.org/cgi/content/full/1090031/DC1
Materials and Methods
Microarray Excel Spreadsheets S1 to S3
References and Notes


4 August 2003; accepted 1 October 2003
Published online 16 October 2003;
10.1126/science.1090031
Include this information when citing this paper.


# REPORTS

## Observation of the Inverse Doppler Effect


**N. Seddon* and T. Bearpark**



**We report experimental observation of an inverse Doppler shift, in which the frequency of a wave is increased on reflection from a receding boundary. This counterintuitive effect has been produced by reflecting a wave from a moving discontinuity in an electrical transmission line. Doppler shifts produced by this system can be varied in a reproducible manner by electronic control of the transmission line and are typically five orders of magnitude greater than those produced by solid objects with kinematic velocities. Potential applications include the development of tunable and multifrequency radiation sources.**


The Doppler effect is the well-known phenomenon by which the frequency of a wave is shifted according to the relative velocity of the source and the observer (*1*, *2*). Our conventional understanding of the Doppler effect, from the schoolroom to everyday experience of passing vehicles, is that increased frequencies are measured when a source and observer approach each other. Applications of the effect are widely established and include radar, laser vibrometry, blood flow measurement, and the search for new astronomical objects. The inverse Doppler effect refers to frequency shifts that are in the opposite sense to those described above; for example, increased frequencies would be measured on reflection of waves from a receding boundary. Demonstration of this counterintuitive phenomenon requires a fundamental change in the way that radiation is reflected from a moving boundary, and, despite a wide range of theoretical work that spans the past 60 years, the effect has not previously been verified experimentally.

Although inverse Doppler shifts have been predicted to occur in particular dispersive media (*3*–*8*) and in the near zone of three-dimensional dipoles (*9*–*11*), these schemes are difficult to implement experimentally and have not yet been realized. However, recent advances in the design of composite condensed media (metamaterials) offers new and exciting possibilities for the control of radiation. In particular, materials with a negative refractive index (NRI) (*12*–*14*) and the use of shock discontinuities in photonic crystals (*15*) and transmission lines


Optics and Laser Technology Department, Advanced Technology Centre, BAE Systems, Post Office Box 5, Filton, Bristol BS34 7QW, UK.

*To whom correspondence should be addressed. E-mail: nigel.seddon@baesystems.com